Bluetooth interference mitigation in 802.11g WLAN

Asif Khan

Reg No 153-FET/MSEE/F08

Supervisor

Dr. Rab Nawaz

Adjunct Faculty,

FET, IIU, Islamabad

Department of Electronic Engineering

Faculty of Engineering and Technology, (FET)

International Islamic University, (IIU), Islamabad.

. Electronic Engineering - Communication
. Detection method - mitigation

Bluetooth interference mitigation in 802.11g WLAN

Asif Khan (153-FET/MSEE/F08)

This dissertation is submitted to Faculty of Engineering and Technology, International Islamic University Islamabad Pakistan for partial fulfilment of the degree of **MS Electronic Engineering** With specialization in **Communication** at the Department of Electronic Engineering

Faculty of Engineering and Technology, (FET)

International Islamic University, (IIU), Islamabad.

Supervisor: Dr. Rab Nawaz

7 Feb 2012

In the name of Allah (SWT) the most benificient and the most merciful.

CERTIFICATE

Title of Thesis: Bluetooth interference mitigation in 802.11g WLAN

Name of Student: Asif Khan

Registration No: 153-FET/MSEE/F08

Accepted by the Faculty of Engineering and Technology, International Islamic University, Islamabad, in partial fulfilment of the requirements for the Master of Philosophy Degree in Electronic Engineering.

Viva voice committee

Dean

Dr. Ghulam Yasin Chohan
FET, IIU , Islamabad

Chairman

Dr. Muhammad Zubair
Assistant Professor,
FET, IIU , Islamabad

External Examiner

Dr. Aqdas Naveed Malik
Professor,
Isra University , Islamabad

Internal Examiner

Dr. Ihsan ul Haq
Assistant Professor
FET, IIU , Islamabad

Supervisor

Dr. Rab Nawaz
Adjunct Faculty,
FET, IIU, Islamabad

21 May 2012

Declaration

I certify that except where due acknowledgments has been made, the work has not been submitted previously, in whole, to qualify for any other academic award, the content of the thesis is the result of work which has been carried out since the official commencement date of the approved research program, and any editorial work paid or unpaid, carried out by a third party is acknowledged.

Asif Khan

153–FET/MSEE/F08

Dedication

TO MY RESPECTED PARENTS WHO HAD WISHED ME WITH THIS DISSERTATION

ABSTRACT

In this thesis, we first propose BT interference modal and then suggest a MUltiple SIgnal Classification or MUltiple SIgnal Characterization (MUSIC) based method to eliminate the effects of Bluetooth (BT) interference upon IEEE 802.11g Wireless Local Area Networks (WLANs). These methods are used for non-coincident interference with 802.11g sub carriers. By exploiting 802.11g preamble we define Difference Term (DT) and give a novel derivation of the MUSIC algorithm for the Difference Terms. MUSIC estimates the interference parameters. We reconstruct interference signal from these estimated parameters. Then, we subtract it from the received time domain signal at channel estimation as well as data decoding stage. We use Bit Error Rate (BER) as a performance metric to show the improvement and perform simulations for a range of interference powers. We show that with the inclusion of our scheme in WLAN receiver, its BER are relatively robust to the BT interference. We have, also, proposed a detection method which tells whether to initiate the mitigation or not. If the eff INR is not good enough we do not go through the mitigation scheme.

ACKNOWLEDGEMENTS

All Praise and Thanks to ALMIGHTY ALLAH, Who gave me the courage and opportunity to carry out this research work. Peace and blessings of Allah be upon His last Prophet Muhammad (Sallulah-o-Alaihihe-Wassalam). All the Knowledge emanates from Almighty Allah.

I offer Sincere thanks to my supervisor **Dr Rab Nawaz** for his able guidance, invaluable support and dynamic supervision throughout the research work. His personal interest and motivation and constructive criticisms resulted in completion of thesis dissertation. He gave me the most needed supervision and took keen interest in Research Paper and thesis with a major impact. He has my deepest respect in both professional and personally

I would like to forward my thanks to my all friend who encouraged me in the successful completion of this dissertation. I would like to mention the great effort of my family specially my parents and brothers who guide and encourage me throughout my life.

Last but not the least; I offer my profound gratitude to those people without whom I could never have accomplished my aim; my family and specially my parents. I thank them all for their constant prayers and determined support throughout this journey.

May Allah Bless you all with endless happiness!

TABLE OF ABBREVIATION

AWGN	Additive White Gaussian Noise
BEP	Bite Error Probability
BER	Bit Error rate
BT	Bluetooth
BIAS	Bluetooth Interference Aware Scheduling
CP	Cyclic Prefix
DMT	Discrete Multi Tone
DFT	Discrete Fourier Transform
DTs	Difference Terms
FFT	Fast Fourier Transform
FH	Frequency Hopping
GFSK	Gaussian Frequency Shift Keying
IFFT	Inverse Fourier Transform

IDFT	Inverse Discrete Fourier Transform
LTF	Long Training Field
MAC	Medium Access Control
NLS	Non linear Least Square
OFDM	Orthogonal frequency Division Multiplexing
PLCP	Physical Layer Convergence Protocol
QOS	Quality of Service
RFI	Radio Frequency Interference
VDSL	Very High Speed Digital Subscriber Line
WLAN	Wireless Local Area Network

TABLE OF NOTATION

i(n)	interference signal
X(k)	training symbols
$x_l(n)$	time domain LTF
V(n)	Additive White Gaussian Noise
H_{ls}	Least Squares (LS) channel estimate
Y	frequency domain received signal
H	channel
V	noise
I	interference
r(n)	received signal
e(n)	sum of the 802.11g signal and the AWGN noise
z(n)	802.11g signal
ω	frequency
α	amplitude
ϕ	phase
d(n)	difference terms
Si	slave
ri	data rate
pi	poll interval
li	packet length
ui	probability of a pair of slots

μi	minimum guaranteed rate
gi	actual rate
ci	compute credits
ωi	compute weights
αi	send factor”,
D	unitary matrix
C	n x n singular matrix
r	covariance matrix
ε	eigenvalues of s3 let that is

TABLE OF CONTENTS

LIST OF FIGURES

LIST OF TABLES

Chapter 1

INTRODUCTION AND MOTIVATION

1.1 Introduction

The bandwidth of 802.11g is 20 MHz. Its physical layer has Orthogonal Frequency Division Multiplexing (OFDM) modulation. An OFDM symbol has duration of 4μs. This may be calculated by using a Cyclic Prefix (CP) of 16 points and a Fast Fourier Transform (FFT) of length 64 [4]. The 802.11g Physical (PHY) layer has preamble, signal and data sections. We can use different lengths of WLAN packets and hence, achieve different data rates. These lengths can be between 40 to 300μs [14].

We have two so called long sequences, known as the Long Training Field (LTF) in the preamble. The channel estimation stage in each packet uses LTF. A CP followed by two identical OFDM symbols makes the LTF [14].

1.2 Bluetooth (BT)

We can easily locate Bluetooth (BT) chips in wireless equipment. They are, for example, printers, audio helmets, cameras, and cars, laptops and PDAs [17].

BT is a member of Wireless Personal Area Networks (WPANs). WPANs are used for low data rates, short-range applications. The modulation used in BT is Gaussian Frequency Shift Keying (GFSK) [6]. Frequency Hopping (FH) is an important characteristic of BT. It can operate (hop) in 79 channels. It has a bandwidth of 1 MHz [6]. A typical WLAN packet is of 2000 bytes if we use its 54 Mbps transmission data rates. The duration of this packet will be 300μsec. If we compare this time with the BT packet times (typically 625 μsec), we may easily conclude that a BT transmission can interfere with the complete WLAN packet. For this interference to occur, of course, the BT should be operating in the frequency band of WLAN [6].

1.3 The WLAN Signal Modal and additive BT interference[14]

In this section, we define the structure of LTF and the remaining WLAN packet. The derivation and the notations are as in [14]. Let us denote the training symbol in frequency domain by X(k), k = 0, 1, . . . , N − 1. We take Inverse Fourier Transform (IFFT) of this training symbol. To construct the CP, we append last P samples of this transform at the start and then put two instances of the inverse transformed signal, itself. The parameter P should be such that P>= 2(L−1). The parameter L represents expected length of the impulse response of the channel. The LTF construction is governed by (1)

$$x_l(n) = \begin{cases} x_l(N+n) & n = 0, \dots, P-1 \\ \frac{1}{\sqrt{N}} \sum_{k=0}^{N-1} X(k)\, e^{j\frac{2\pi k(n-P)}{N}}, & n = P, \dots\dots, P+N-1 \\ x_l(n-N) & n = P+N, \dots, 2N+P-1 \end{cases} \quad (1)$$

In this thesis, we assume a time-invariant multipath Rayleigh fading channel [4]. The received signal *r(n)* will be written as

$$r(n) = \sum_{\tau=0}^{L-1} \mathrm{h}(\tau) x_l(n-\tau) + \mathrm{v(n)} + \mathrm{i(n)} \quad (2)$$

where *n* ranges from 0 to 2N+P-1.

In the above Equation (2), v(n) represents Additive White Gaussian Noise (AWGN) whose variance is σ_v^2. The BT interference signal is represented by i(n). The first step in channel estimation is to discard first P samples of $r(n)$. Then we perform an N-point FFT of the next N samples in the received signal.

We know that a convolution in time domain is multiplication in frequency domain. Therefore, the whole procedure can be represented in frequency domain as

$$Y = XH+V+I \tag{3}$$

where Y is the frequency domain received signal, H represents frequency domain channel response, V represents noise in frequency domain, and I is the frequency domain transform of the BT interference.

We have our training symbol X(k) at the main diagonal of X which is an N × N diagonal matrix. The channel is estimated using the Least Square (LS) formula

$$H_{ls} = X^{-1}Y \tag{4}$$

Equation (4) is also applied to the second length N instance of X(k). The two channel estimates are averaged to reduce the effects of additive AWGN noise.

Note that, at the data decoding stage of the WLAN packet, we will need this channel estimate. The data will be decoded using

$$X = H_{ls}^{-1}Y \tag{5}$$

This method of channel estimation as well as data decoding will be referred to as 'LS' in our simulations.

We see in Equation (3) above that I component is a problem for both channel estimation as well as data decoding stages. As our simulations will show LS method degrades in the presence of this interference component.

1.4 Motivation[15]

We have shown in the previous section that BT interference is a problem for proper WLAN reception. Because, of above explained degradation, there are retransmissions by the WLAN transmitter, or the WLAN systems lowers its data rates. This impact of course depends upon the relative power levels of WLAN and BT. Though the power levels of BT are low compared to WLAN, the power of WLAN is spread over its sub-carriers and individual subcarriers are susceptible to interference. An example situation is when we are using a laptop to connect to printers, PDAs using BT and to connect to Internet using WLAN. We need solutions that allow both technologies to work together without interfering with each other.

The following Figure shows narrow band BT interference for the 802.11g WLANs.

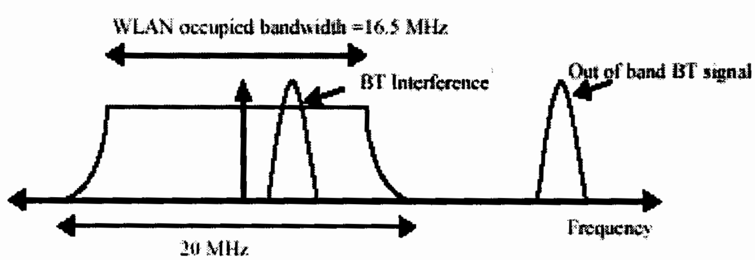

Figure: 1.1 BT interference for the 802.11g WLANs.

<u>2.4 GHz (802.11b/g/draft-n) channel frequencies[16]</u>

Channel	frequency (MHz)	North America	Japan	Most of world
1	2412	Yes	Yes	Yes
2	2417	Yes	Yes	Yes
3	2422	Yes	Yes	Yes
4	2427	Yes	Yes	Yes
5	2432	Yes	Yes	Yes
6	2437	Yes	Yes	Yes
7	2442	Yes	Yes	Yes
8	2447	Yes	Yes	Yes
9	2452	Yes	Yes	Yes
10	2457	Yes	Yes	Yes
11	2462	Yes	Yes	Yes
12	2467	No	Yes	Yes
13	2472	No	Yes	Yes
14	2484	No	.11b only	No

Table 1: **2.4 GHz (802.11b/g/draft-n) channel frequencies**

BT Channel Frequencies [17]

Country	Frequency Range	RF Channels	
Europe* & USA	2400 - 2483.5 MHz	f = 2402 + k MHz	k= 0,...,78
Japan	2471 - 2497 MHz	f = 2473 + k MHz	k= 0,...,22
Spain	2445 - 2475 MHz	f = 2449 + k MHz	k= 0,...,22
France	2446.5 - 2483.5 MHz	f = 2454 + k MHz	k= 0,...,22

Table 2: **BT Channel Frequencies [17]**

Note that if for example we are using WLAN channel#4 in North America centred at frequency 2427 MHz, the BT channels from 2402 MHz to 2480 MHz may or may not centre at the WLAN subcarriers. This is because one BT channel is 1 MHz while WLAN subcarriers are approximately 0.3 MHz apart. We conclude that there are two types of the BT interference for the 802.11g WLAN systems.

- Sub carrier coincident interference -> Frequency of the BT interference coinciding with the 802.11g sub carrier frequencies.
- Sub carrier non-coincident interference -> Frequency of the BT interference not coinciding with the 802.11g sub carrier frequencies.

BT interferes with few WLAN subcarriers due to its narrow bandwidth. The Signal to Interference Ratio (SIR) is therefore different on different subcarriers. Due to FFT leakage effects, if the BT interference is non-coincident, it affects a large number of subcarriers, though the effect decreases as we move away from the centre of the interference. If it is coincident, it mainly affects 3 subcarriers coz of 1 MHz bandwidth.

1.5 Outline of Thesis

The remaining chapters outline is provided below.

Chapter#02:

This chapter explores literature to find methods for mitigation of Bluetooth interference in WLAN. This chapter, in particular, describes modified Non linear Least Square (NLS) method [14].

Chapter#03

The proposed algorithm is detailed in this chapter. The chapter gives algorithm derivation. It also defines an eff INR measure which shows the margin of improvement of the proposed approach from the LS method.

Chapter#04

This chapter describes the simulation environment. Matlab is used to simulate the algorithms and compare their performance. The simulations results are explained with detailed comments.

Chapter #05

We give our final comments and conclusions in this chapter. Some future directions are also identified.

Chapter 2

LITERATURE SURVEY

The solutions to the BT interference can be divided into two groups.

Collaborative Mechanisms

where some form of communication exists between WLAN and Bluetooth (BT). This link can be used to provide fair sharing of medium. Note that by these methods, we the two systems cannot cooperate at their best data rates.

Non-Collaborative Mechanisms:

where no communication between WiFi and Bluetooth exists. Techniques are developed to minimize the effects of the mutual interference so that both systems can cooperate and give their best data rates. [15].

Medium Access Control (MAC) layer cooperative methods are proposed in [3] which in fact try to avoid collision of WLAN and BT transmitted packets. A natural consequence is that these methods result into lowering the data rates of either of WLAN or BT [4].

Method proposed by [5] suggests replacing those WLAN symbols whose sub carriers are near the BT transmission by erasures. The authors in [6] propose to weight the reliability metrics corresponding to the bits of a sub carrier according to their respective SIRs. These methods assume that the WLAN receiver can estimate the BT frequency, though this would require a BT receiver embedded into the WLAN receiver. As we mention in the conclusions, our proposed approach can serve to locate the BT interference for these methods, too.

If the interference is always present in a known frequency band, method proposed in [7] can be used. This method places null tones in the expected interference band and uses the received signal on these null tones to infer about the interference. Due to the hopping of BT transmission, the interference is not always present in a known band and such techniques are not applicable.

The paper by Lin [18] assumes an AWGN channel model which is an oversimplification. In case of AWGN channel, the problem becomes too simple. Becasue at channel estimation stage, you will just subtract the training symbols in the frequency domain and will get the V+I signal. At the data decoding stage, just subtract this V+I signal and get your symbols. We simulate more realistic scenario by assuming multipath channel modal.

2.1 Modified NLS algorithm [14]

The non-coincident BT interference was dealt with in [14]. The authors propose to deal with the interference in Physical layer of the 802.11g systems. The authors proposed a BT interference modal and suggest estimating the BT interference and subtracting it from the received WLAN signal, before the data decoding stage. This counters the BER degradation of the WLAN receivers in the presence of BT interference. Modified NLS algorithm [3], explained in the next section, was employed for the BT interference parameters estimation.

The BT interference modal suggested in [14] can be mathematically described as

$$i(n) = \sum_{k=1}^{3} a_k \, e^{j(\omega_k n + \varphi_k)} \qquad (6)$$

n=0,1,2,...

This modal consists of three complex sinusoids whose frequencies are separated by one subcarrier width. The angular frequency $\omega_k = 2\pi f_k$, while we represent the 3 complex sinusoids amplitudes and frequencies by α_k ,and φ_k The φ_k's are defined to be independent random variables and they are distributed uniformly in the range $[-\pi, \pi)$.

We know that the subcarrier frequencies of 802.11g are given by f_k; $k = 0, 1/N, \ldots, (N-1)/N$. We may encounter coincident BT interference in which case the interference will exactly center the subjected subcarrier. For non-coincident BT interference, the interference will not center the subcarrier. For example, the authors in [14] set $f1 = 27/N$; $f2 = 28/N$; $f3 = 29/N$ for a BT interference centered at 29th 802.11g subcarrier. For non-coincident, they set $f1 = 27.2/N$; $f2 = 28.2/N$; $f3 = 29.2/N$.

We suggest to modal non-coincident interference with a single complex sinusoid at a partial frequency as it is difficult to assume that now the interference will only be located at three partial frequencies. When the non-coincident sinusoid is added it affects the surrounding subcarriers, too, due to the leakage of the FFT. We show a BT interferer of frequency 34.5/N in the Figure 2.

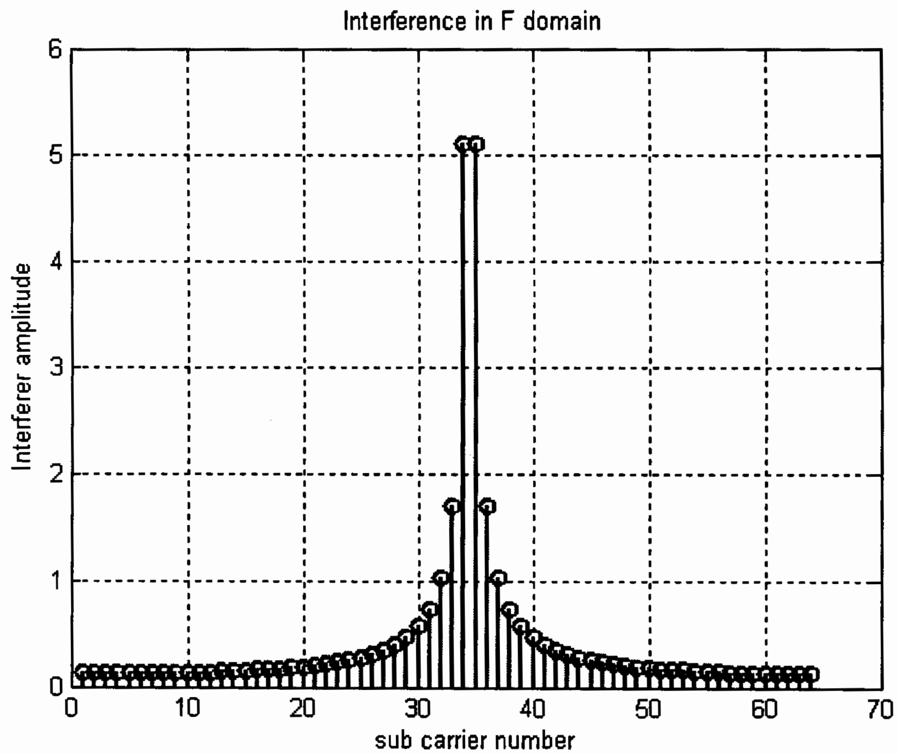

Figure 2: BT interference at non-coincident frequency of 33.5/N

In the following, we go through the derivation of the NLS algorithm for the estimation of the BT interferer parameters.

2.2. Modified Non linear Least Square (MNLS [14])

We will describe the derivation in [14] to show the steps for the estimation of the frequency of the interference using modified NLS algorithm. The amplitude and phase estimation is trivial once frequency estimates have been made. We can write (2) as

$$r(n) = z(n) + v(n) + i(n)$$

$$= i(n) + [z(n) + v(n)] \qquad (7)$$

$$= i(n) + e(n) \qquad n = 0, \dots, \bar{N} - 1 \qquad (8)$$

$\bar{N} = 2N + P$ represents the number of samples in the LTF. For frequency estimation, the sum of 802.11g signal z(n) and AWGN noise manifest as the error signal *e(n)*. The parameters are estimated by minimizing the following [12]

$$J(\omega, \alpha, \phi) = \sum_{n=0}^{\bar{N}-1} \left| r(n) - \alpha e^{j(\omega(n)+\varphi)} \right|^2 \qquad (9)$$

We define

$$\beta = \alpha e^{j\varphi}$$

$$\mathbf{r} = [r(0), \dots, r(\bar{N} - 1)]^T$$

$$\mathbf{b} = [1 \; e^{jw} \; \dots \; e^{jw(\bar{N}-1)}]^T$$

we can write (9) as

$$J = (\mathbf{r} - \mathbf{b}\boldsymbol{\beta})^H(\mathbf{r} - \mathbf{b}\boldsymbol{\beta})$$

$$\hat{\omega} = \arg\max_w[\mathbf{r}^H\mathbf{b}(\mathbf{b}^H\mathbf{b})^{-1}\mathbf{b}^H\mathbf{r}] \qquad (10)$$

Once the frequency is estimated, we can get least square estimates of α and φ by using [12]

$$\hat{\beta} = (\mathbf{b}^H\mathbf{b})^{-1}\mathbf{b}^H\mathbf{r}\Big|_{\omega=\hat{\omega}} \qquad (11)$$

Difference Terms (DTs):

We can see that 802.11g signal consists of a sum of sinusoidal. Therefore the received signal cannot directly be used to estimate the BT interferer parameters. Therefore, we need to get rid of the 802.11g signal z(n) from the received signal in (7), if we want to estimate parameters of the sinusoidal interference. The special structure of the LTF gives us the following interesting result

$$z(n) = z(n + N), \quad n = L - 1, L, \ldots, P + N - 1 \qquad (12)$$

This applies as long as $P \geq L-1$. Here we define a derived signal known as the Difference Terms (DTs)

$$d(n) = r(n + L - 1 + N) - r(n + L - 1), \qquad (13)$$

$$n = 0, 1, \ldots, P + N - L$$

we have in the sequel

$$d(n) = \bar{\iota}(n) + \bar{v}(n)$$

$$= \alpha e^{j(\omega(n+L-1)+\varphi)}(e^{j\omega N)} - 1) + \bar{v}(n) \tag{14}$$

Where $\bar{v}(n) = v(n + L - 1 + N) - v(n + L - 1)$. This signal now represents zero mean complex AWGN. Due to the difference operation its variance is doubled ($2\sigma_v^2$) than the variance of the original additive noise [21] , n = 0, 1, . . . , P + N – L. The NLS method will be modified to use DTs. Equations (10)-(11) will be used to estimate ω, α, and ϕ but will use $\mathbf{d} = [\mathbf{d}(0), \mathbf{d}(1), \ldots, \boldsymbol{d}(P + N - L)]^T$ instead of $\mathbf{r}$. The vector **b** will also change to b_d given as

$$\mathbf{b_d} = [e^{j\left(\omega(\bar{I}+L-1)\right)}(e^{j\omega N} - 1)]^T \tag{15}$$

$$\bar{I} = 0, \ldots, P + N - L + 1.$$

We have successfully eliminated OFDM signal in **d** so that now modified NLS algorithm will estimate parameters of the interference in a much cleaner environment. By cleaner, we mean the additive noise for the interference estimation will be additive not colored. The interference signal is reconstructed using the parameters estimated by the above algorithm. We subtract the reconstructed signal from our received signal in the time domain. Now the interference is mitigated and we can perform the FFT for channel estimation.

The same procedure is adopted at the data decoding stage. The authors in [14] use P = 2L in the preamble. We shall simulate this method for comparison with our approach. We note that the DTs have been mentioned in [19]. Unfortunately we cannot have DTs samples more than CP – (L – 1). We get these samples in between OFDM symbols of WLAN packet. This number is not adequate for interference parameter estimation except at the channel estimation stage where the CP is of doubled length than the standard CP used between every OFDM symbol in a WLAN packet and we get adequate number of consecutive DT samples. The authors in [19] assume CP equal to the length of FFT which is impractical as it will greatly reduce the bandwidth efficiency of OFDM.

The complexity of the NLS algorithm in general is very high. For multiple BTs present, the frequency search will be prohibitively large. Therefore, we propose to use subspace based methods to estimate the BT frequency. We show that our proposed method is as robust as NLS algorithm for the interference modal assumed. The additional benefits of the subspace based method are mentioned in the conclusions in chapter 5.

Chapter 3

Proposed Mitigation Algorithm

Modified MUSIC algorithm

Here we shall give a novel derivation of the MUSIC algorithm. The MUSIC is a high resolution algorithm which is used to estimate frequency of sinusoidal in noise. The Modified MUSIC algorithm will estimate the frequency of a sinusoidal using Difference Terms (DTs).

3.1. Eigen decomposition of the Autocorrelation Matrix of the Difference Terms (DTs)

We proposed the BT interference modal in chapter 2. Our mitigation scheme necessitates the estimation of the additive complex exponential parameters i.e., its frequency, amplitude and phase.

For frequency estimation, we propose to use the autocorrelation matrix of the DTs. Once the frequency is estimated, the amplitude and phase can be estimated using NLS method used in the previous chapter.

The eigendecomposition of the autocorrelation matrix based methods are well documented in [21]. These methods eigendecompose the autocorrelation matrix into two subspaces, a signal subspace and a noise subspace. We shall use the noise subspace methods in this thesis.

Note that we are using the DTs, not the actual values of a sinusoid. Therefore the derivation will be modified accordingly.

The autocorrelation sequence of the DTs is

$$r_d(k) = P_1 F_1 e^{jk\omega_1} + 2\sigma_v^2 \delta(k), \quad P_1 = |\alpha_1|^2, \quad F_1 = 2[1 - \cos(\omega_1 N)] \tag{16}$$

Note the inclusion of F_1 term due to the nature of DTs. An m x m autocorrelation matrix R_d will be given as

$$R_d = R_s + R_v \tag{17}$$

Where $\mathbf{R}_s$ and $\mathbf{R}_v$ are the autocorrelation matrices due to signal and noise, respectively.

We have

$$R_s = P_1 F_1 \begin{bmatrix} 1 & e^{-j\omega 1} & e^{-j2\omega 1} & \cdots & e^{-j(m-1)\omega 1} \\ e^{j\omega 1} & 1 & e^{-j\omega 1} & \cdots & e^{-j(m-2)\omega 1} \\ e^{j2\omega 1} & e^{j\omega 1} & 1 & \cdots & e^{-j(m-3)\omega 1} \\ \vdots & \vdots & \vdots & & \vdots \\ e^{j(m-1)\omega 1} & e^{j(m-2)\omega 1} & e^{j(m-3)\omega 1} & \cdots & 1 \end{bmatrix} \tag{18}$$

Which has a rank one and

$$R_v = 2\sigma_v^2 I \tag{19}$$

Is diagonal and has full rank.

Note that if we define

$$e_1 = [1\ e^{j\omega 1}\ e^{j2\omega}\ \cdots\ e^{j(m-1)\omega 1}]^T \tag{20}$$

Then

$$R_s = P_1 F_1 e_1 e_1^H \tag{21}$$

And

$$R_s e_1 = P_1 F_1 (e_1 e_1^H) e_1 = P_1 F_1 e_1 (e_1^H e_1) = m P_1 F_1 e_1 \tag{22}$$

Therefore, $\mathbf{e_1}$ is the eigenvector of $\mathbf{R_s}$. The corresponding eigenvalue is mP_1F_1. Since $\mathbf{R_s}$ is Hermitian, all its other eigenvectors are orthogonal to $\mathbf{e_1}$ [21],

$$e_1^H v_i = 0\ ; i = 2,3,\cdots,m \tag{23}$$

Finally, if we let λ_i^s to be the eigenvalue of $\mathbf{R_s}$ then

$$R_d v_i = (R_s + 2\sigma_v^2 I) v_i = \lambda_i^s v_i + 2\sigma_v^2 v_i = (\lambda_i^s + 2\sigma_v^2) v_i \tag{24}$$

Therefore, by definition, the eigenvectors of $\mathbf{R_s}$ and $\mathbf{R_d}$ are the same.

The largest eigenvalue of $\mathbf{R_d}$ is $(mP_1F_1 + 2\sigma_v^2)$ and the remaining (m-1) eigenvalues are equal to $2\sigma_v^2$.

Let $\mathbf{v_i}$ be the noise eigenvectors of $\mathbf{R_d}$, then

$$\widehat{P} e^{jw} = \frac{1}{\sum_{i=2}^{m} |e^H v_i|^2} = \frac{1}{\sum_{i=2}^{m} \left|\sum_{k=0}^{m-1} v_i(k) e^{-jk\omega 1}\right|^2}$$

(25)

The denominator is the summation of the Fourier transform of the individual noise eigenvectors. By orthogonality principal mentioned in Equation (23), the denominator should be equal to zero at $w=w_1$. Then $\hat{P}e^{jw}$ will be large (in theory infinity) at $w=w_1$. This method is called MUltiple SIgnal Classification (MUSIC). The method in its original derivation assumes p sinusoids. In our case $p=1$.

Another alternative MUSIC formulation is called root MUSIC. The z-transform of each noise eigenvector i.e., the *eigenfilter* has *(m-1)* roots. Ideally one of them will lie on the unit circle at the frequency of the complex exponential.

$$V_i(z) = \sum_{k=0}^{m-1} v_i(k) z^{-k} \quad i= 2, \cdots m-1 \tag{26}$$

And we can use all *eigenfilters* corresponding to all the noise eigenvectors as under

$$D(z) = \sum_{i=2}^{m} V_i(z) V_i^*(1/z^*) \tag{27}$$

Our frequency estimate will be the angle of the root of the polynomial D(z) that is closest to the unit circle. It sometimes helps because now we look at angle not the magnitude

3.2 Coincident vs Non-coincident Interference

We may mention here that the DTs have non-zero samples only if the BT interference is non-coincident. The Figure 3 shows F_1 values for BT frequencies between any two (normalized) subcarrier frequencies of 802.11g. We see that F1 is zero at the BT frequencies coincident with the WLAN frequency. We also see that except for 0.1 and 0.9 locations, F_1 has values greater than 1. Therefore the matrix Rs will be zero for coincident frequencies, and there is no question of frequency estimation using the eigendecomposition approach.

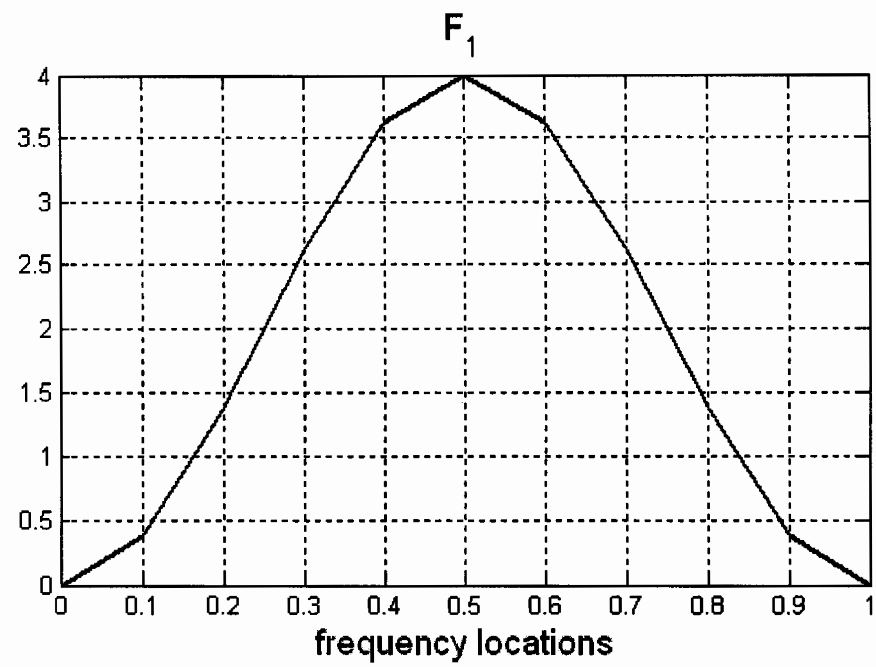

Figure 3: F1 term supporting the middle frequencies.

3.3 Effective INR: A metric for mitigation initiation

As already noted the largest eigenvalue of $\mathbf{R_d}$ is $mP_1F_1 + 2\sigma_v^2$ and the remaining (m-1) eigenvalues are equal to $2\sigma_v^2$. If we subtract the average of these m-1 eigenvalues from the largest eigenvalue and divide the result by m, we get $P_1 F_1$. Therefore we propose the following criterion called Effective Interference to Noise Ratio (eff INR)

$$\text{Eff INR} = \frac{\lambda_1 - \text{mean}(\lambda_2, \ldots, \lambda_m)}{m * \text{mean}(\lambda_2, \ldots, \lambda_m)} = \frac{mP_1F_1 + 2\sigma_v^2 - 2\sigma_v^2}{m * 2\sigma_v^2} = \frac{mP_1F_1}{m * 2\sigma_v^2} = \frac{P_1F_1}{2\sigma_v^2} \tag{28}$$

Therefore the autocorrelation matrix $\mathbf{R_s}$ will have its contribution in $\mathbf{R_d}$ as compared to $\mathbf{R_v}$ if *eff INR* is high.

We will come back to this phenomenon in the simulations chapter.

Chapter 4.

PERFORMANCE ASSESSMENT

4.1. Simulations

The simulation environment used is similar to that of [14]. We simulate 10^4 packets. Each packet has independent realization of data, channel, noise and interference. Each packet consists of 32 OFDM symbols. We employ QPSK constellation. Gray coding is used at the transmitter which is relatively robust to noise. The simulated multipath channel is assumed to have delay spread of 50ns (rms value). This translates into L=11 taps using Fs=20 MHz [4]. We normalize the channel in our simulations. The modified NLS method uses a step size of 0.1 Hz for the grid search. The preamble in the LTF has P=22 samples. We separate the timing and frequency synchronization issues and assume that these have already been performed by using the starting portion of preamble.

We define $$S = 10\log_{10}(X^2) = 10\log_{10}(1) \qquad (29)$$

$$SNR = 10\log_{10}\left(\frac{1}{\sigma_v^2}\right) \qquad (30)$$

where ${\sigma_v}^2 = E\{|v(n)|^2\}$ denotes the noise variance. SIR is defined as $SIR = 10\log_{10}\left(\frac{1}{\alpha^2}\right)$ where α is the BT sinusoid amplitude. Note that in these definitions, by signal we mean the WLAN signal. Therefore, for SNR=20 dB and SIR=10 dB, the Interference to Noise Ratio (INR) would be 10 dB using the formula

$$\mathrm{INR} = \mathrm{SNR} - \mathrm{SIR} \qquad (31)$$

We simulate interference at different non-coincident frequencies. We do it for $f = \frac{16.1}{N}, \frac{16.3}{N}, \frac{16.5}{N}, \frac{16.7}{N}, \frac{16.9}{N}$, in our simulations, similarly we do it for $f = \frac{33.1}{N}, \frac{33.3}{N}, \frac{33.5}{N}, \frac{33.7}{N}, \frac{33.9}{N}$ and $f = \frac{53.1}{N}, \frac{53.3}{N}, \frac{53.5}{N}, \frac{53.7}{N}, \frac{53.9}{N}$. Our algorithm performance depends also upon m. We perform simulations for different values of m. We finally select m=50 as it gives best MSE and BER performance. The values of SIR= -30, -20, -10, 0, 10, 15 dB. As we use negative to positive SIRs, we are simulating near to far BT inference situated near to far from the WLAN receiver.

'LS' curves represent the channel estimation and data decoding without interference mitigation. The 'Ref' curves represent the MSE and BER calculations without the BT contamination in the WLAN signal.

4.2 SIMULATION RESULTS

The figures (4) and (5), respectively show the BER and MSE curves for the LS, Ref, and the MUSIC algorithm for BT non-coincident frequencies of 16.1, 16.3, 16.5, 16.7 and 16.9 versus the SNR. We see that the proposed MUSIC algorithm outperforms the LS algorithm. The MSE and BER curves are very close to the Ref curve. The value SIR was -20dB. Therefore, we can read INR on the x-axis by just adding 20 dB for each simulated SNR value. Therefore, these simulations represent INR from 20 to 60 dB. The MSE curves in Figure (4) for frequencies 16.1 and 16.9 show odd behavior. It was expected as explained in the previous chapter. The F_1 term reduces effective INR for these frequencies. As the plot of F1 term suggest, we do not see this degradation of INR for other frequency locations. We will explain the effect of small eff INR on the MSEs by the end of this chapter. These curves begin to outperform the LS curve from SNR of 5 dB (INR of 25 dB) and onward, though.

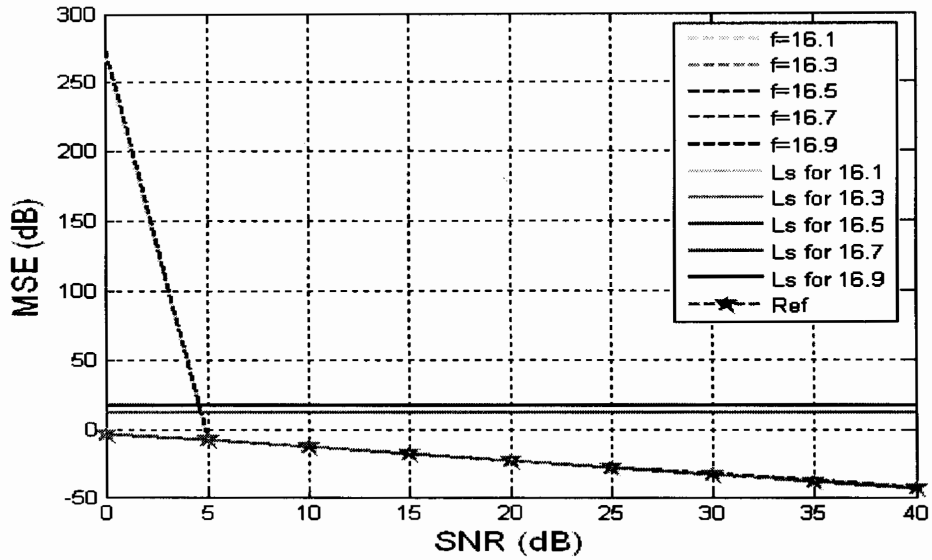

Figure: 4 MSE curves for the LS, Ref, and the MUSIC algorithm for BT non-coincident frequencies of 16.1, 16.3, 16.5, 16.7 and 16.9 versus the SNR .

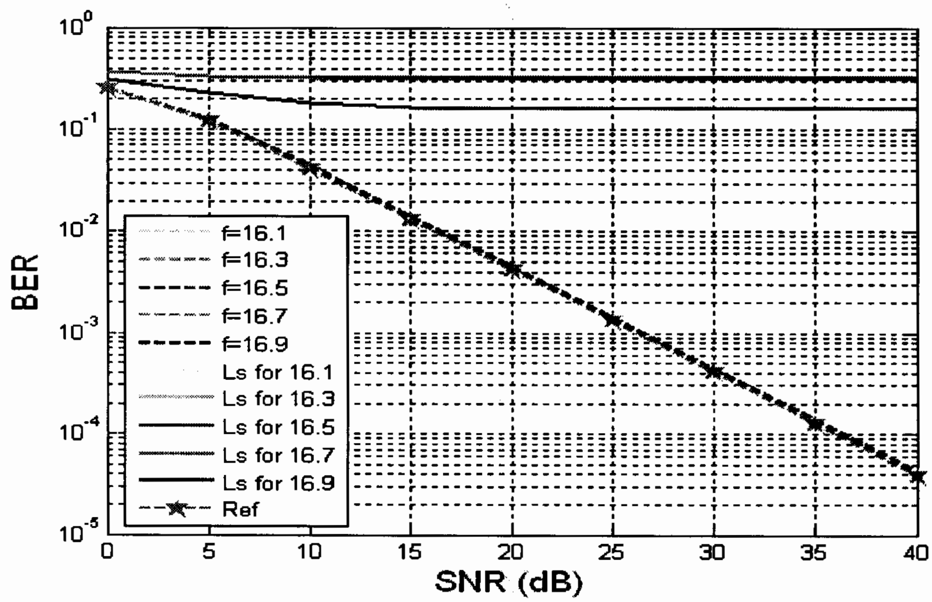

Figure: 5 BER curves for the LS, Ref, and the MUSIC algorithm for BT non-coincident frequencies of 16.1, 16.3, 16.5, 16.7 and 16.9 versus the SNR.

The figure (6) and (7), respectively show the MSE and BER curves for the LS, Ref, and the NLS algorithm for BT non-coincident frequencies of 16.1, 16.3, 16.5, 16.7

and 16.9 versus the SNR. The value SIR was -20dB. We see that the NLS algorithm also outperforms the LS algorithm similarly as our proposed MUSIC based algorithm did. The MSE and BER curves are very close to the Ref curve. The MSE curves in Figure (6) for frequencies 16.1 and 16.9 show odd behavior. It shows that the NLS algorithm has the MSE degradation due to low INR similar our algorithm.

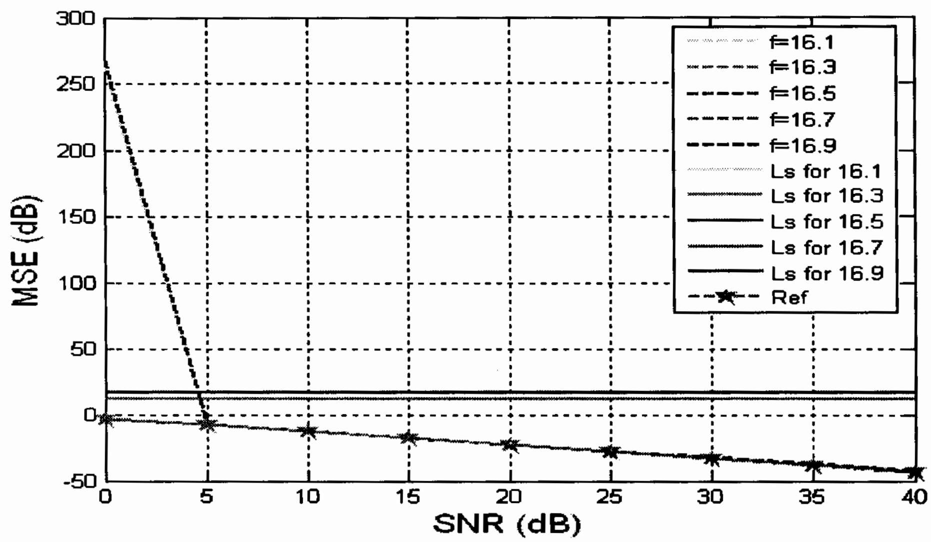

Figure: 6 MSE curves for the LS, Ref, and the NLS algorithm for BT non-coincident frequencies of 16.1, 16.3, 16.5, 16.7 and 16.9 versus the SNR

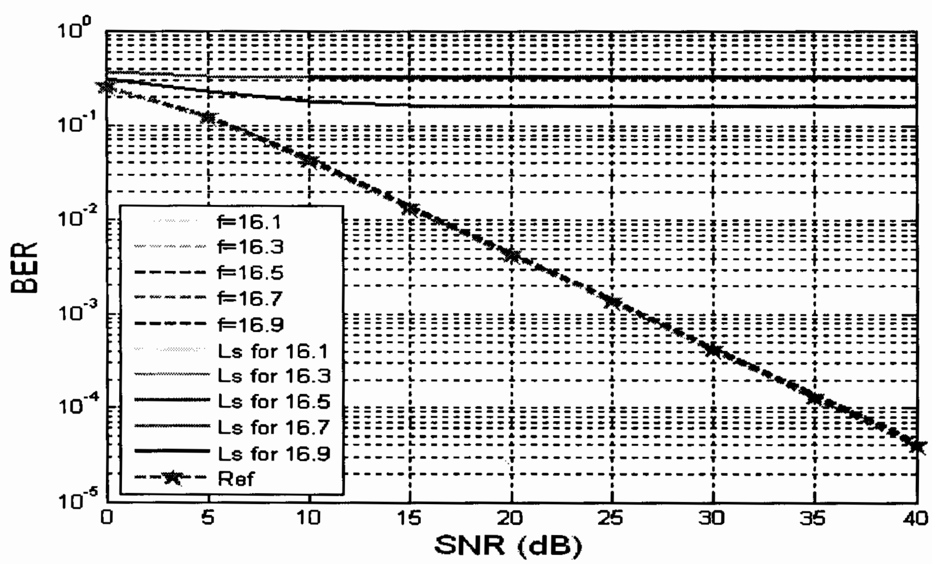

Figure: 7 BER curves for the LS, Ref, and the NLS algorithm for BT non-coincident frequencies of 16.1, 16.3, 16.5, 16.7 and 16.9 versus the SNR

The figures (8) and (9), respectively show the BER and MSE curves for the LS, Ref, and the MUSIC algorithm for BT non-coincident frequencies of 33.1, 33.3, 33.5, 33.7 and 33.9 versus the SNR. We see that the proposed MUSIC algorithm outperforms the LS algorithm. The MSE and BER curves are very close to the Ref curve. The value SIR was -20dB. Therefore, we can read INR on the x-axis by just adding 20 dB for each simulated SNR value. Therefore, these simulations represent INR from 20 to 60 dB. The MSE curves in Figure (9) for frequencies 16.1 and 16.9 show odd behavior. It was expected as explained in the previous chapter. The F_1 term reduces effective INR for these frequencies. As the plot of F1 term suggest, we do not see this degradation of INR for other frequency locations. We will explain the effect of small eff INR on the MSEs by the end of this chapter. These curves begin to outperform the LS curve from SNR of 5 dB (INR of 25 dB) and onward, though.

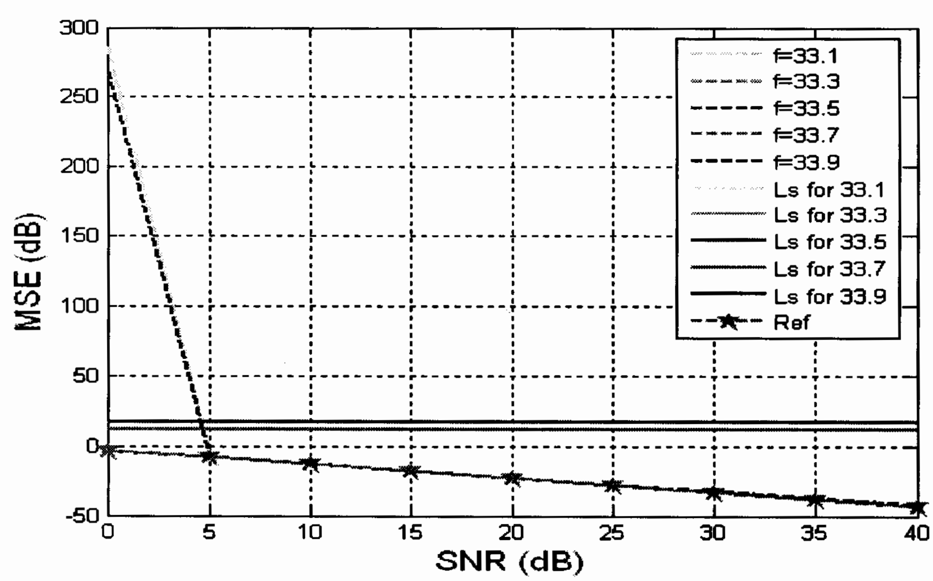

Figure: 8 MSE curves for the LS, Ref, and the MUSIC algorithm for BT non-coincident frequencies of 33.1, 33.3, 33.5, 33.7 and 33.9 versus the SNR.

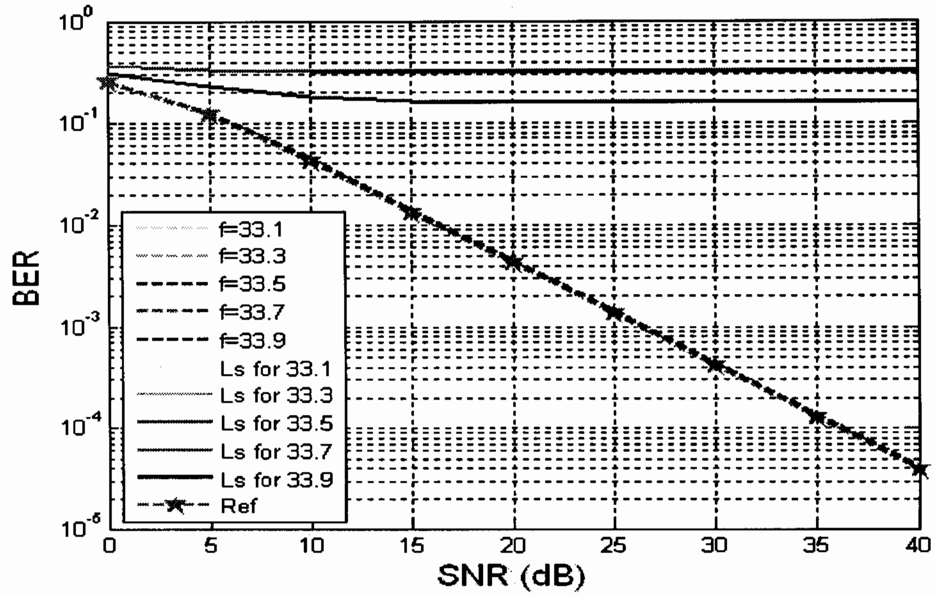

Figure: 9 BER curves for the LS, Ref, and the MUSIC algorithm for BT non-coincident frequencies of 33.1, 33.3, 33.5, 33.7 and 33.9 versus the SNR.

The figure (10) and (11), respectively show the MSE and BER curves for the LS, Ref, and the NLS algorithm for BT non-coincident frequencies of 33.1, 33.3, 33.5, 33.7 and 33.9 versus the SNR. The value SIR was -20dB. We see that the NLS algorithm also outperforms the LS algorithm similarly as our proposed MUSIC based algorithm did. The MSE and BER curves are very close to the Ref curves. We can read INR on the x-axis by just adding 20 dB for each simulated SNR value. Therefore, these simulations represent INR from 20 to 60 dB. The MSE curves in Figure (10) for frequencies 33.1 and 33.9 show odd behavior. It shows that the NLS algorithm has the MSE degradation due to low INR similar our algorithm.

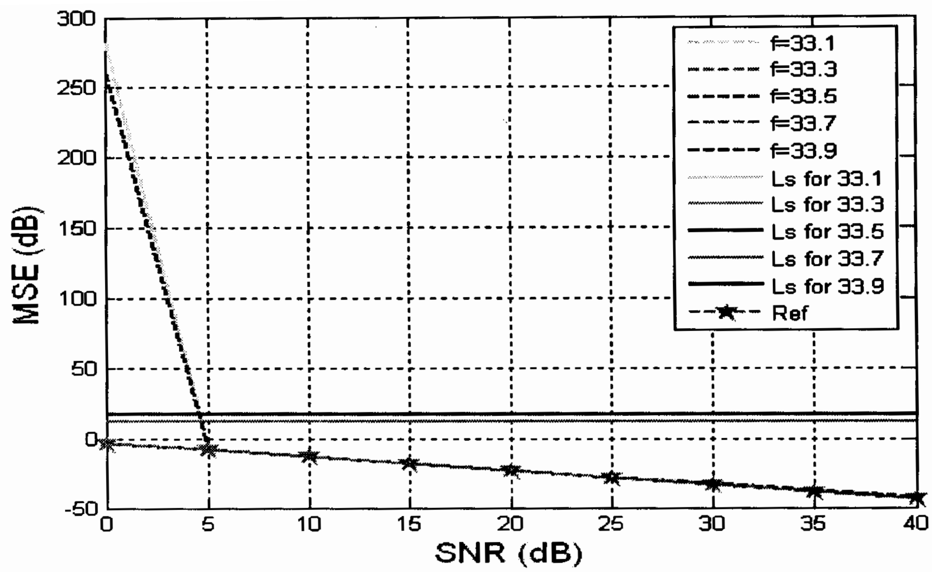

Figure: 10 MSE curves for the LS, Ref, and the NLS algorithm for BT non-coincident frequencies of 33.1, 33.3, 33.5, 33.7 and 33.9 versus the SNR

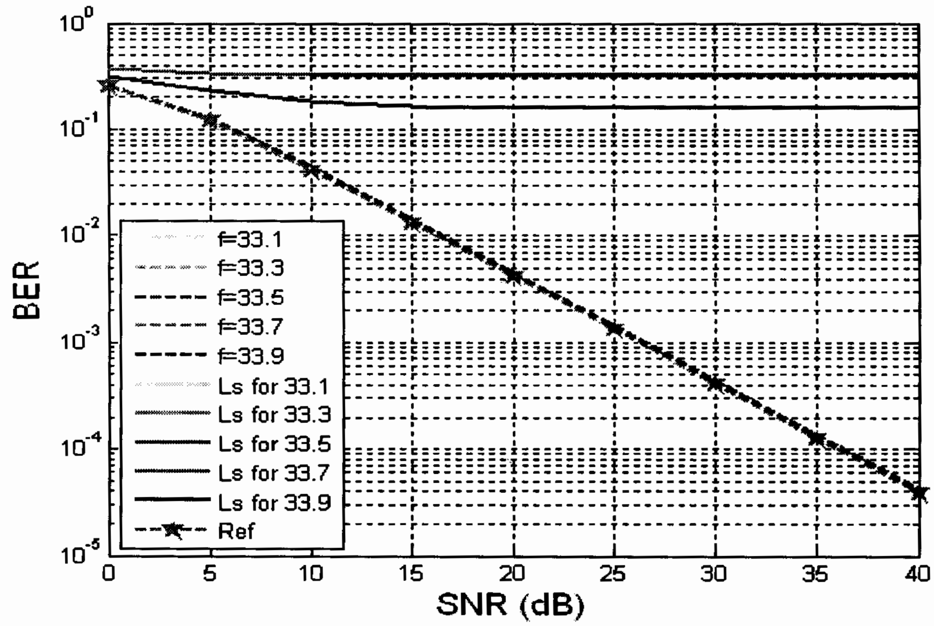

Figure: 11 BER curves for the LS, Ref, and the NLS algorithm for BT non-coincident frequencies of 33.1, 33.3, 33.5, 33.7 and 33.9 versus the SNR

The figures (12) and (13), respectively show the BER and MSE curves for the LS, Ref, and the MUSIC algorithm for BT non-coincident frequencies of 53.1, 53.3, 53.5, 53.7 and 53.9 versus the SNR. We see that the proposed MUSIC algorithm outperforms the LS algorithm. The MSE and BER curves are very close to the Ref curve. The value SIR was -20dB. Therefore, we can read INR on the x-axis by just adding 20 dB for each simulated SNR value. Therefore, these simulations represent INR from 20 to 60 dB. The MSE curves in Figure (12) for frequencies 53.1 and 53.9 show odd behavior. It was expected as explained in the previous chapter. The F_1 term reduces effective INR for these frequencies. As the plot of F1 term suggest, we do not see this degradation of INR for other frequency locations. We will explain the effect of small eff INR on the MSEs by the end of this chapter. These curves begin to outperform the LS curve from SNR of 5 dB (INR of 25 dB) and onward, though.

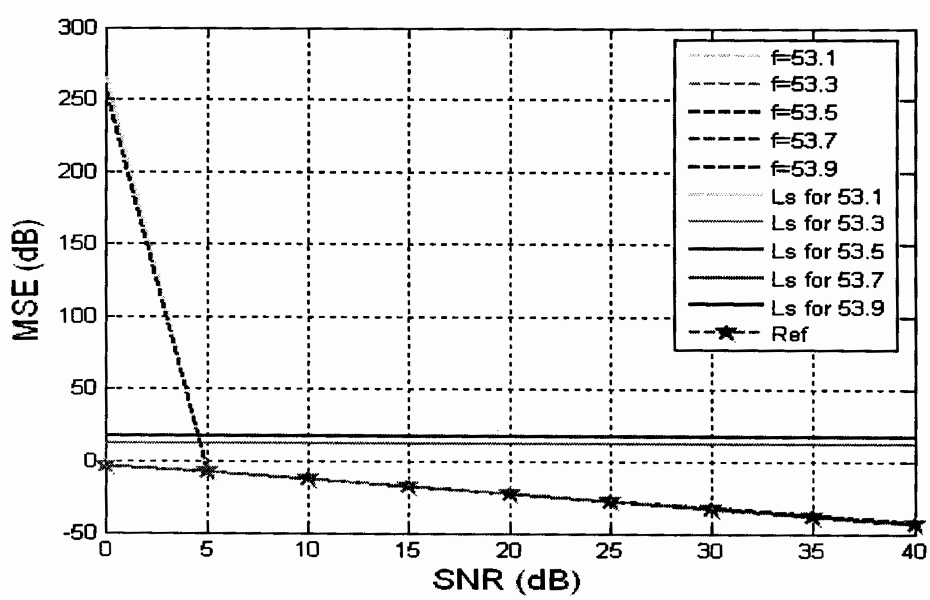

Figure: 12 MSE curves for the LS, Ref, and the MUSIC algorithm for BT non-coincident frequencies of 53.1, 53.3, 53.5, 53.7 and 53.9 versus the SNR

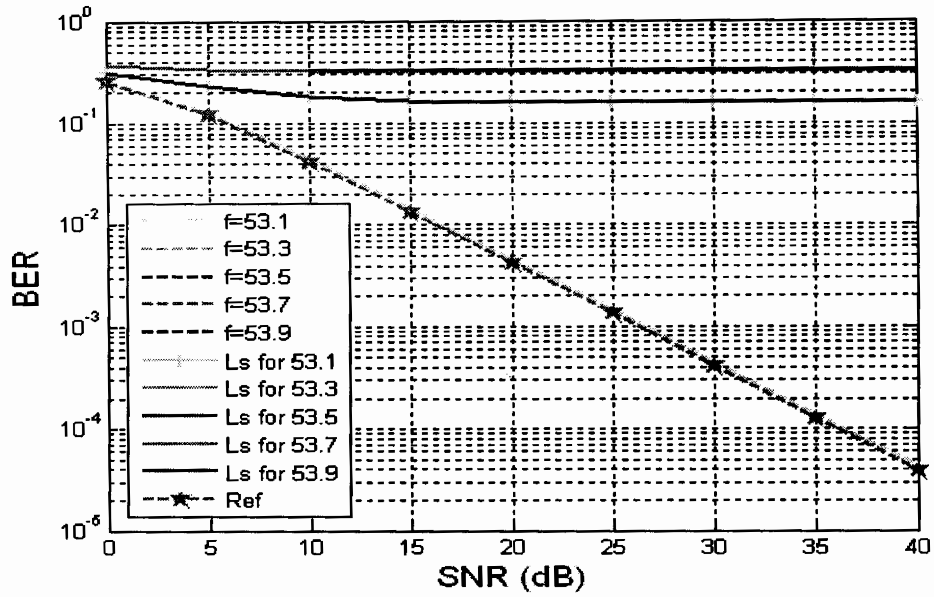

Figure: 13 BER curves for the LS, Ref, and the MUSIC algorithm for BT non-coincident frequencies of 53.1, 53.3, 53.5, 53.7 and 53.9 versus the SNR

The NLS results for frequencies of 53.1, 53.3, 53.5, 33.7 and 53.9 versus the SNR were similar. We have not included here for brevity.

As was shown in previous figures (12, 13) our proposed MUSIC based algorithm is robust to the BT interference present around any normalized frequency of the WLAN signal band. Therefore our proposed approach solves the BT interference problem for majority of frequency locations.

The figure (14) and (15), respectively show the MSE and BER curves for the LS, Ref, and the proposed algorithms for SIRs of -30, -20, -10, 0, 10, and 15 dB versus the SNR. The value of non-coincident frequency was 33.3. We see that the proposed MUSIC algorithm outperforms the LS algorithm. Its MSE and BER curves are very close to the Ref curve. We can read INR on the green curve corresponding to the SIR of 0 dB as the same as SNR. We see that the proposed approach outperforms LS only after INR is greater than 5 Db.

We can read INR on the blue curve corresponding to the SIR of 10 dB as from -10 to 30 dB on the x-axis. Interestingly, again, we see that the proposed approach outperforms LS only after INR is greater than 5 Db. Now the point where MSE curve come close to the Ref curve has shifted to SNR=15 dB. It means that for the same frequency location, and support of F1 term, we need more support from SNR for a weak interference.

We can read INR on the magenta curve corresponding to the SIR of 15 dB as from -15 to 25 dB on the x-axis. Interestingly, again, we see that the proposed approach outperforms LS only after INR is greater than 5 Db. Now the point where MSE curve come close to the Ref curve has shifted to SNR=20 dB. It means that for the same frequency location, and support of F1 term, we need even more support from SNR for a weak interference.

4.3 <u>Low Eff INR</u>

The detailed analysis of the algorithm results shows that when the eff INR is not good enough, the algorithm often estimates coincident frequencies. We know that for coincident frequencies, the DTs do not contain any useful signal. Therefore, when the algorithm wrongly estimates the frequency to be coincident for the DTs provided, its amplitudes estimates diverge and it gives too high amplitudes. We see amplitude estimates in the order of 10^{28}.

Note that the frequencies of 0.1 and 0.9 locations have a negative impact on the INR due to F_1 term. Secondly the chances of wrongly estimation of a coincident frequency are more for these frequencies, too. These were the reasons we saw degradation particularly in their MSE in the previous figures. In the current Figures, though the frequency of the SIR is 33.3 but its power is low against SIR=10 dB. Therefore, at low SNR locations, the eff INR becomes low and we see the similar degradation in the MSEs.

When the interference mitigation subtracts a very high amplitude sinusoid of an exact frequency, it gives rise to a very high MSE. As far as the BER curve is concerned, it is degraded similar to LS curve as their BERs are similar. We may comment that this is noise dominant zone. We see relatively less degradation from the Ref curve, though.

Note that when we put SIR to be positive, we are introducing low value for P1. To keep the eff INR sufficient, and hence raise contribution of the matrix $\mathbf{R_s}$ as compared to $\mathbf{R_v}$, we need to lower the noise power. We know from the previous chapter that

$$Eff\ INR = \frac{P_1 F_1}{2\sigma_v^2}$$

Of course, F1 supports the non-coincident frequencies at locations 0.3, 0.5, 0.7 more than those at 0.1 and 0.9. It means that for supported frequencies, we will start having marginal performance from the LS algorithm from a lower SNR.

We may threshold the eff INR to infer the margin of improvement we can have with our mitigation scheme. If the strength of the interference is small, LS will be less degraded, P1 will give rise to a small eff INR and hence we will know that the margin of improvement is small. At higher SNRs, the LS algorithm flattens, but small σ_v^2 gives rise to large eff INR, we have large margin of performance.

For all other curves, the INR reads from 10 dB and onward. Therefore, we do not see any degradation in the MSE curves versus the LS curve.

For practical SNRs ranging from (20-40) dB, we see that our proposed algorithm outperforms the LS algorithm from very weak BT interference (SIR=10 Db) to strong BT interference (SIR = -30 dB).

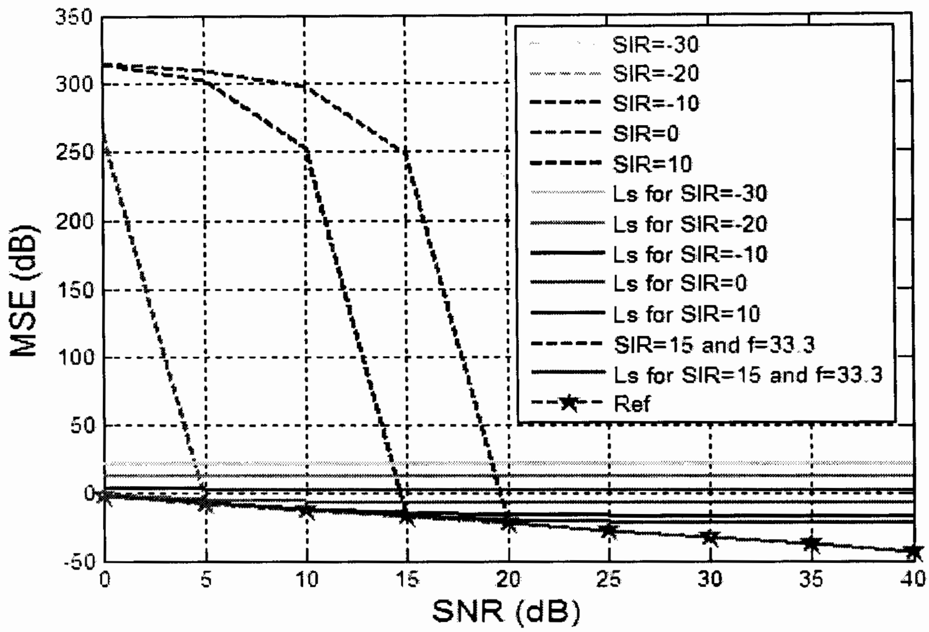

Figure: 14 MSE curves for the LS, Ref and the proposed algorithms for SIRs of -30, -20, -10, 0, 10, and 15 dB versus the SNR

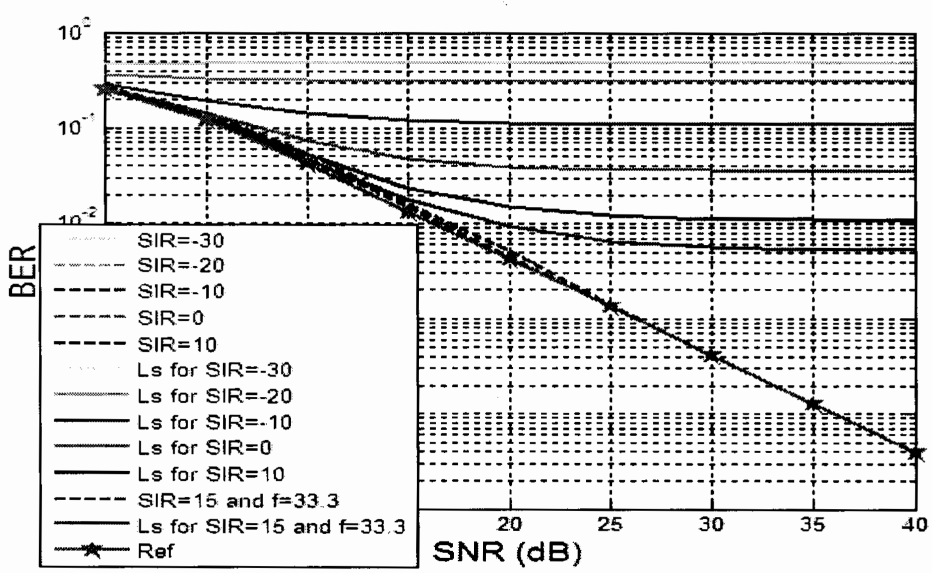

Figure: 15 BER curves for the LS, Ref and the proposed algorithms for SIRs of -30, -20, -10, 0, 10, and 15 dB versus the SNR

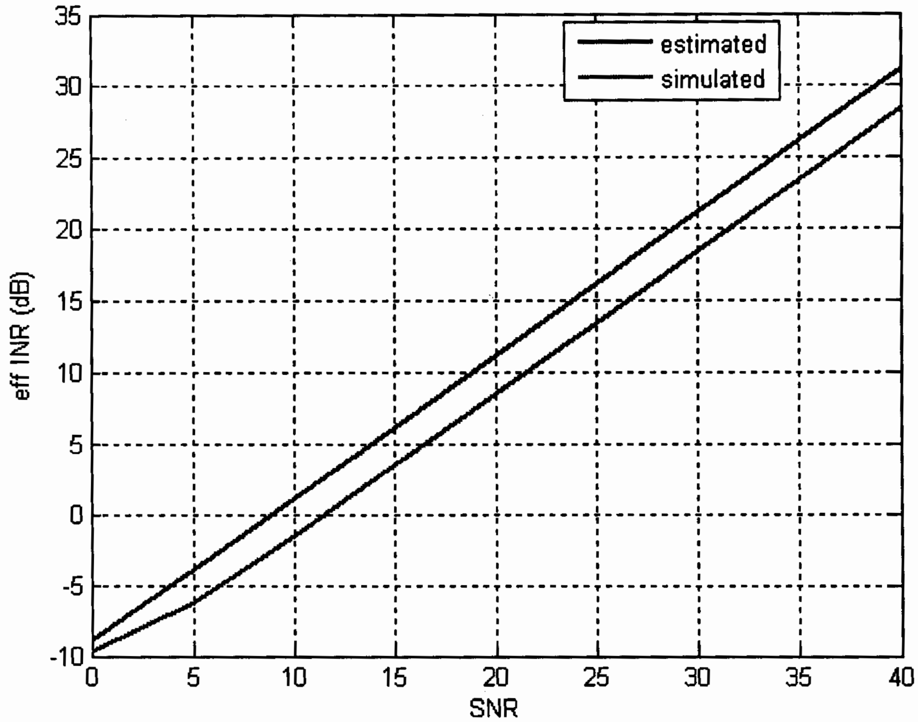

Figure 16: Eff INR and its simulated values for BT at 33.3 and SIR=10 dB

Figure (16) shows the plots of eff INR and its simulated values for BT frequency at 33.3 with SIR=10 Db. The two curves approximately agree with our proposed formula for eff INR. By looking at this Figure and the one showing BERS, we see that the margin of improvement is substantial for eff INRs greater than 10 dB.

In above two figures, it seems that BER curves for the proposed algorithm are always lower than the LS curves. It shows that the degradation by the LS algorithm is always worse than that of the proposed approach whatever the INR might be. This is very important result. It means our proposed approach can be a silent component of the WLAN receiver and will always safeguard against the BT interference in terms of BER OR it may be initiated once the INR exceeds a threshold to get marginal performance.

Chapter 5.

CONCLUSIONS AND FUTURE WORK

5.1 Conclusions

The following conclusions can be drawn from the previous chapters

- We have solved BT interference for the WLANs as majority of locations around sub-carriers are covered now except coincident interference.
- A novel derivation of the MUSIC algorithm for DTs has been provided.
- The use of DTs helps estimate the interference parameters for mitigation and get BERs as if there was no interference present.
- We have proposed a novel detection method based on effective INR which tells whether to initiate the mitigation or not. If the eff INR is not good enough we do not go through the mitigation scheme.

5.2 Future Work

- The proposed method can be used for the mitigation of multiple BT interferences. The CC does not grow with multiple sinusoids as in NLS. Moreover, It not only detects presence of interference but gives idea of how many interferes are present. In NLS you have to tell beforehand the number of interferers.
- For erasure based methods, our method locates the interference so that the subcarriers under the influence of interference are known. Due to its

amplitude estimation, you may also decide how many subcarriers should be subjected to erasures.

References

[1] "Draft supplement to 802.11-1999, Wireless LAN MAC and PHY specifications: Further Higher-Speed Physical Layer (PHY) extension in the 2.4 GHz band," in IEEE 802.11g/D2.1, http://standards.ieee.org/catalog/olis/lanman.html.

[2] K. V. S. S. S. S. Sairam, N. Gunasekaran, and S. R. Reddy, "Bluetooth in wireless communication", IEEE Commun. Mag., vol. 40, no. 6, pp. 90–96, June 2002.

[3] N. Golmie, N. Chevrollier, and I. ElBakkouri, "Interference aware Bluetooth packet scheduling", in IEEE Globecom., vol. 5, pp. 2857–2863, Nov. 2001.

[4] M. Ghosh and V. Gaddam, "Bluetooth interference cancellation for 802.11g WLAN receivers", in IEEE Int. Conf. Commun., vol. 2, pp. 1169–1173, May 2003.

[5] K. K. Wong and T. O'Farrel, "Coverage of 802.11g WLANs in the presence of bluetooth interference", in 14th IEEE Int. Symp. Personal, Indoor and Mobile Radio Commun., vol. 3, pp. 2027–2031, Sep. 2003.

[6] A. K. Arumugam, A. Doufexi, A. R. Nix, and P. N. Fletcher, "An investigation of the coexistence of 802.11g WLAN and high data rate Bluetooth enabled consumer electronic devices in indoor home and office environments", IEEE Trans. Cons. Elec., vol. 49, no. 3, pp. 587–596, Aug 2003.

[7] F. Sjoberg, R. Nilsson, P. O. Borjesson, P. Odling, B. Wiese and J. A. C. Bingham, "Digital RFI suppression in DMT-based VDSL systems", IEEE Trans. Circuits and Sys.-I, vol. 51, no. 11, pp. 2300–2312, Nov. 2004.

[8] P. Stoica and R. Moses, "Introduction to Spectral Analysis. Upper Saddle River", N.J.: Prentice Hall, 1997.

[9] "Coexistence of Wireless Personal Area Networks with other wireless devices operating in unlicensed frequency bands", in IEEE 802.15.2-2003, http://ieeexplore.ieee.org/servlet/opac?punumber=8755.

[10] J. W. Ketchum and J. G. Proakis, "Adaptive algorithms for estimating and

suppressing narrowband interference in PN spread-spectrum systems" , IEEE Trans. Commun. and Sys.-I, vol. COM-30,no. 5, pp. 913–924, May 1982.

[11] A. Parekh and R. Gallager, "A generalized processor sharing approach to flow control - the single node case" , in ACM/IEEE Transactions on Networking, June 1993, vol. 1, pp. 344–357.

[12] P. Stoica and R. Moses, "Introduction to Spectral Analysis" ,Upper Saddle River, N.J :PrenticeHall , 1997.

[13] D. Bertsekas and R. Gallager," Data Networks", 2nd Ed., Prentice Hall,1992.

[14] R. Nawaz and S. Sun, "Bluetooth Interference mitigation in 802.11g", in IEEE Int. Conf. Commun.,May 2008.

[15] http://www.wi-fiplanet.com/tutorials/article.php/1379911

[16] http://en.wikipedia.org/wiki/List_of_WLAN_channels

[17] http://linuxwireless.org/en/users/Documentation/Bluetooth-coexistence

[18] Shi-Qing Lin, Lei Xia, Jin Hua and Shao-Qian Li, "Iterative Interference Suppression Algorithm Based on EST", National Key Laboratory of Science and Technology on Communications University of Electronic Science and Technology of China Cheng du, China

[19] Rab Nawaz and Sumei Sun, "Channel Estimation in 802.11g in the presence of Bluetooth Interference", Institute for Infocomm Research, A* STAR, Singapore.

[20] C. de Frein, M. Flanagan, and A. Fagan, "OFDM narrowband interference estimation using cyclic prefix based algorithm", in 11th International OFDM Workshop, http://ee.ucd.ie/~mark/papers/OFDM Workshop NBI.pdf, Hamburg, Germany, Aug. 2006.

[21] Monson H Hayes, "Statistical digital signal processing and modeling".

[22]H.Labiod Int ,"Wi-Fitm Tm,Bluetooth Zig Bee and Wimax" , Evry, France Enst, Paris, France H.Afifi C .De Santis Int, Evry, France Wi-Fitm Tm,

[23] Xiao-Jiao Tao , "Bluetooth-WiFi Coexistence in Mobile Handset", April-2009